

Decoupled Sparse Priors Guided Diffusion Compression Model for Point Clouds

Xiaoge Zhang¹ Zijie Wu² Mehwish Nasim¹ Mingtao Feng³ Ajmal Mian¹
¹ The University of Western Australia ² Hunan University ³ Xidian University

Abstract

Lossy compression methods rely on an autoencoder to transform a point cloud into latent points for storage, leaving the inherent redundancy of latent representations unexplored. To reduce redundancy in latent points, we propose a sparse priors guided method that achieves high reconstruction quality, especially at high compression ratios. This is accomplished by a dual-density scheme separately processing the latent points (intended for reconstruction) and the decoupled sparse priors (intended for storage). Our approach features an efficient dual-density data flow that relaxes size constraints on latent points, and hybridizes a progressive conditional diffusion model to encapsulate essential details for reconstruction within the conditions, which are decoupled hierarchically to intra-point and inter-point priors. Specifically, our method encodes the original point cloud into latent points and decoupled sparse priors through separate encoders. Latent points serve as intermediates, while sparse priors act as adaptive conditions. We then employ a progressive attention-based conditional denoiser to generate latent points conditioned on the decoupled priors, allowing the denoiser to dynamically attend to geometric and semantic cues from the priors at each encoding and decoding layer. Additionally, we integrate the local distribution into the arithmetic encoder and decoder to enhance local context modeling of the sparse points. The original point cloud is reconstructed through a point decoder. Compared to state-of-the-art, our method obtains superior rate-distortion trade-off, evidenced by extensive evaluations on the ShapeNet dataset and standard test datasets from MPEG group including 8iVFB, and OwlII.

1. Introduction

Point clouds are the most common raw form of 3D data representation and are widely used for representing objects or scenes in various applications such as mixed reality [25], autonomous driving [35], and object reconstruction [33]. With the rapid advancement of 3D acquisition technology, complex geometries can now be captured in real time as large point clouds that offer detailed geometric information.

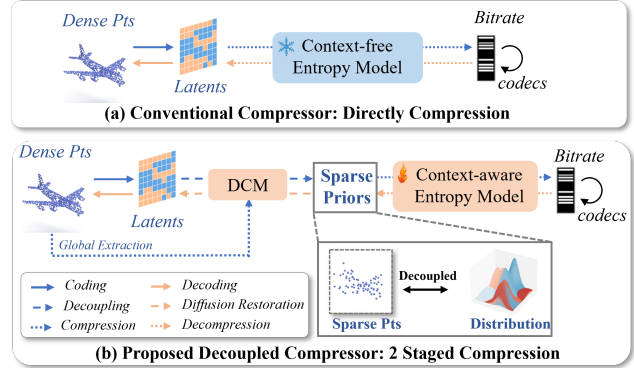


Figure 1. (a) Conventional compressors code the latent representation of points directly via a naive context-free entropy model. (b) Our method codes the sparse priors via a context-aware entropy model. It employs a two-stage data flow to compress the points further into decoupled sparse priors, and incorporates a progressive attention-based conditional diffusion model to denoise the latent representations conditioned on the sparse priors.

However, this poses considerable challenges for storing and transmitting such large volumes of data, highlighting the need for more efficient point cloud compression techniques that minimize storage footprint while maintaining geometric fidelity.

Lossy geometry compression methods can be divided into voxel-based and point-based methods. Both employ an encoder to map a point cloud or voxels into low-dimensional latent points as well as attached features, which we call *latents* briefly unless otherwise specified. The latents are then coded into a binary string using an entropy model for storage, and the decoder reconstructs the original point cloud from the decoded latents. Voxel-based methods [18, 29] transform point clouds into voxels before applying established image compressors to acquire latent codes. These methods take advantage of extensively validated image compression techniques but suffer from heavy computational overhead and geometry loss due to voxelization. Despite attempts Wang et al. [28] to reduce memory by sparse convolution [5], these networks struggle with high sparsity, leading to inadequate local context. Point-based methods typically utilize an auto-encoder structure, as shown in Fig. 1(a). Yan et al. [34] and Huang and Liu [12] pro-

pose to directly compress the raw point cloud data in the latent space, with the latent representations extracted by existing backbone networks such as PointNet [22] or PointNet++ [23]). However, the decompressed point clouds tend to lose local details making it difficult to balance the compression rate and reconstruction quality. Recently, He et al. [8] proposed a density-aware encoder to retain local density by enforcing density loss. However, this method suffers from rapid degradation of neighboring information as the compression ratio increases, limiting its effectiveness to scenarios with lower compression ratios.

To achieve efficient compression while preserving fine-grained details, we propose a sparse priors guided diffusion compression model. This model introduces a dual-density data flow to remove the redundancy within the latents, leveraging a compact hierarchical representation to maximize the compression of the overall geometry and higher-fidelity latents to faithfully reconstruct the original structure. The sparse points, which are downsampled at a higher rate, act as a more compact version of the latent representation, capturing the overall structure while summarizing the collapsed points that surround the sparse points and are discarded during downsampling. The sparse priors encode the relationships within the collapsed set around each sparse latent point, though it leaves the spatial dependencies between the sparse latent points themselves unexplored. To address this limitation, we model each sparse latent point as a composite of local factors, including underlying surfaces, curvature, and point density. A lightweight predictor is then used to learn an adaptive local distribution based on the geometry and context of neighboring points, enabling a more efficient representation of intra-point relationships over a broader receptive field.

To retain geometry integrity of the sparse cues, we propose a diffusion compression model (DCM) that leverages a progressive attention-based denoiser (PACD) to generate fine-grained latents, which aggregates the sparse cues by an efficient fusion block. The PACD effectively captures the inherent variability and uncertainty in the latent space, ensuring that a rich and diverse distribution of both geometric and semantic information is fed to the decoder. Simultaneously, it maintains the completeness and accuracy of the original point cloud geometry while minimizing storage costs, as the diffuser is guided by homogeneous data.

By employing two distinct encoding streams and utilizing the DCM as an intermediary, our framework separates the latents used for reconstruction from the sparser representations used for storage. This separation enables more flexible size constraints on the latents, while ensuring high reconstruction fidelity, even under high compression ratios. Additionally, to better exploit the intra-point priors, we integrate the local distribution into a context-aware entropy model, thereby improving the binary encoding of

sparse points. This approach contrasts with the conventional context-free entropy model, which assumes a global distribution.

Our main contributions can be summarized as follows:

- We propose a lossy point cloud compression data flow that compresses a point cloud further into *sparse priors*. By capitalizing on the form simplicity of sparse priors, we relax the size constraints imposed on latents for reconstruction and reduce the inherent redundancy.
- We introduce a multi-stage sparsity guided conditional diffusion scheme. We decouple the sparse priors into inter-point sparse latents and intra-point local distributions, and employ progressive cross-attention to aggregate priors from both scales across varying downsampling rates. The sparse mapping is learned jointly with the denoising process to preserve consistent topological and semantic properties with the original point cloud.
- We present a decoupled sparse priors guided diffusion compression model (DSP-DCM) for point cloud, driven by conditional diffusion model and context-aware entropy model. Our framework denoises the latent representations conditioned on the sparse priors, enabling the generation of high-quality distribution-enhanced structures even at extremely low bitrates. Our inter-point local distribution is also integrated into both the arithmetic encoder and decoder to enhance the contextual modeling of sparse points.

Experiments on the ShapeNet and standard MPEG test datasets (8iVFB, OwlII) validate that our method achieves a state-of-the-art rate-distortion performance.

2. Related Work

2.1. Point Cloud Compression

Voxel-based methods [18, 19] first voxelize and partition the input point cloud and then feed the cubes to a 2D convolution neural network. To reconstruct the original point cloud, the topologic relationship between the cubes is also stored with negligible bits. VoxelDNN [18] uses a ResNet backbone to predict the occupancy probability distribution of voxels, which suffers from low encoding and decoding speeds as both processes work in a sequential fashion. To alleviate this problem, MSVoxelDNN [19] proposes to predict the distribution in a coarse-to-fine order. For lossy point cloud compression, [24, 30] treats the mapping from latent representations to original voxels as a binary classification problem. [24] learns a 3D auto-encoder consisting of an analysis transform, an entropy model for binary compression, and a synthesis transform, which has become a standard pipeline for lossy voxel-based compression. Wang [29] proposed to predict the mean and variance of latent representations to enhance the coding contexts. Voxel-based methods struggle with imbalanced distributions of voxel oc-

cupancy in sparse point clouds and incur high overhead with dense point clouds. In contrast, our method compresses point sets directly, enhancing scalability for dense point clouds while reducing sensitivity to sparsity.

Octree-based methods transform a point cloud into an octree with predetermined number of layers, and then an MLP-based network predicts the distribution of non-leaf nodes. Since each non-leaf node has eight children, the compression can be formulated as a classification of 256 categories. OctSqueeze [11] was the first to introduce learnable octree-based point cloud compression. It employs multiple MLP layers to predict the occupancy probabilities of child nodes based on information from parent or ancestor nodes. By encoding nodes layer-by-layer, the method allows for simultaneous encoding of multiple nodes within each layer. Similar in concept to OctSqueeze, OctAttention [6] improves node context by incorporating information from nodes within the same layer, achieving high accuracy in probability distribution predictions. However, it experiences slow decompression speeds because non-leaf nodes depend on their siblings despite the use of local window parallelism. EHEM [27] is proposed as a solution to this problem. EHEM splits the nodes into two disjoint groups; the first is independent of sibling nodes and the other group just relies on the first group in terms of information from the same layer. This allows for the simultaneous inference of all nodes within a group strategy and greatly shortens the decoding time. Compared to voxel-based methods, octree-based methods are more efficient in terms of runtime and memory usage. However, they remain sensitive to point distribution and are less suited for dynamic contexts due to the high maintenance costs associated with hierarchical structures.

Point-based methods D-PCC [8] directly process the geometry by an auto-encoder [9]. The encoder reduces the point cloud resolution via down-sampling and encodes it into a compact binary format using a bottleneck entropy model. The decoder then reconstructs the full point cloud from the compressed format. The method’s performance degrades at high compression ratios due to substantial loss of neighboring information. To address this, we introduce a decoupled data flow that preserves sparse points while employing latent points for point cloud reconstruction. This approach effectively generates high-quality, distribution-enhanced structures, even at extremely low bitrates.

2.2. Diffusion for Point Cloud Analysis

The diffusion model was first proposed for image generation [10, 26] and has gradually been applied to various tasks for point cloud analysis in recent years. [14] is the first to leverage diffusion model for unconditional point cloud generation. Zhou et al. [37] designs a neural network that combines point and voxel representations for point cloud

completion. Wu [33] proposes to utilize sketches and texts as conditions to generate object-level colored point clouds. This approach involves fusing sketch and point cloud features through a cross-attention mechanism, with separate diffusion models generating geometry and appearance information. Point-E [20] employs diffusion models to create three-dimensional shapes from images by fine-tuning GLIDE models with specific language prompts. [16] resorts diffusion model to generate object-level meshes. The first diffusion model generates dense point cloud conditioned on sparse point cloud while the second diffusion model generates corresponding features from dense point cloud, after feeding a point-wise auto-encoder with both geometry and attribute data to reconstruct the point cloud, surface reconstruction is employed to generate the mesh. In our method, diffusion models capture complex data distributions and reduce noise, effectively mitigating data loss from high compression rates.

3. Proposed Approach

As depicted in Fig. 2, the proposed DSP-DCM separately processes latent representations and sparse priors, augmented by a progressive latent diffusion model guided by the sparse priors. To effectively compress the original point cloud X , we address the inherent redundancy within latent points X_L and attached features F_L by using a dual-density data flow in Sec 3.1, which consists of two separate encoders: point encoder Θ_L and sparse encoder Θ_S . These encoders generate (X_L, F_L) and sparse points (X_S, F_S) ensuring that $|X_S| < |X_L|$, while storing only the latter. For simplicity, we will use \mathbf{X}_S to denote the sparse point cloud X_S along with associated features F_S . Likewise, \mathbf{X}_L will refer to the pair (X_L, F_L) in the remainder of the discussion unless otherwise specified. To complement data loss during downsampling, we also predict the local distribution (μ_S, σ_S) for each sparse point as inter-point priors. For high-fidelity reconstruction during decompression in Sec 3.2, we condition the latent denoiser \mathcal{D} progressively on the sparse priors, \mathbf{X}_S and (μ_S, σ_S) , to preserve low-frequencies and deterministic aspects of the original structure. Subsequently, the predicted latents $\tilde{\mathbf{X}}_L$ are fed to a point decoder to reconstruct high-quality point cloud X . Additionally, in Sec 3.3, the learned local distribution is also integrated into the entropy model \mathcal{E} to improve contextual modeling of sparse points during binary coding.

3.1. Decoupled Sparse Prior Guided Data Flow

Our DSP-DCM comprises two stages, *sparse coding* and *prior decoupling*, while the first stage encodes the original point cloud into dual-density representations, latents and decoupled sparse prior, the second stage adopts a progressive attention-based conditional diffuser (PACD) to generate high fidelity latents based on hierarchical cues. The first

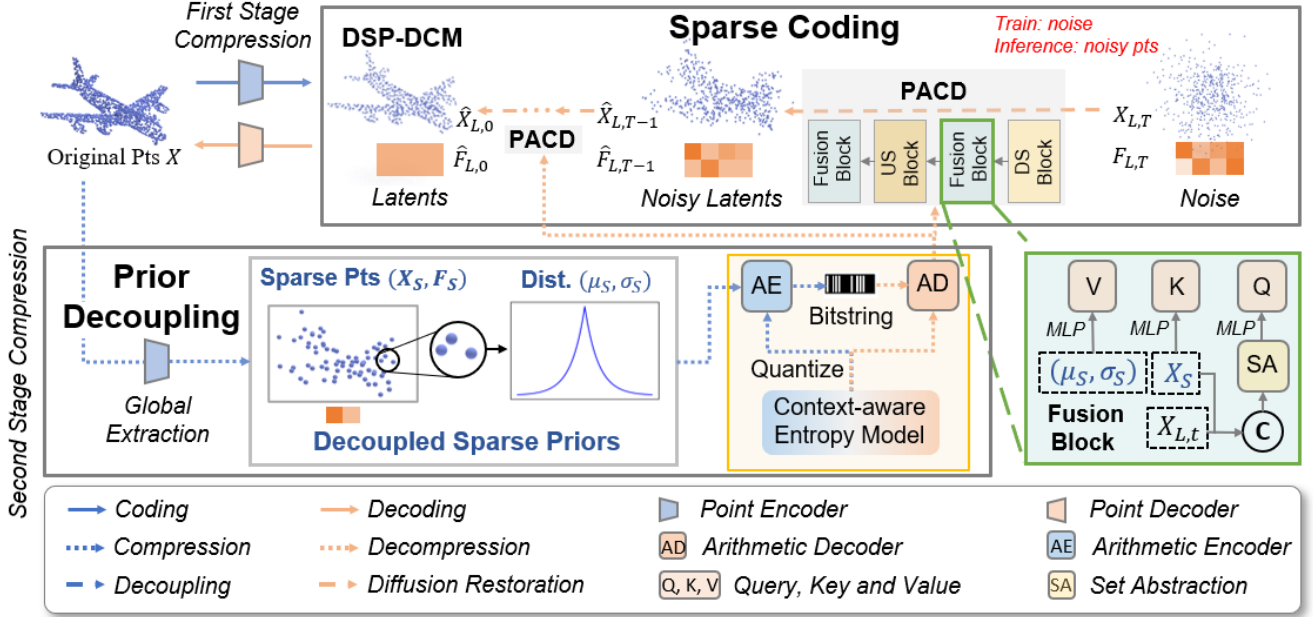


Figure 2. Overview of our decoupled sparse priors guided diffusion compression model for point cloud (DSP-DCM). Our approach begins with a point encoder that transforms the input point cloud into latent points and features. Instead of directly encoding these latents, we extract sparser representations obtained through a separate sparse encoder. The DCM further decouples the sparser representation into sparse points and intra-point local distributions. During decompression, we start with Gaussian noise and apply a progressive attention-based conditional denoiser (PACD) on the sparse point cloud to reconstruct the latents. These reconstructed latents are then decoded to produce a high-quality point cloud.

stage is to scatter the spatial structure and preserve a compact manifestation of the original point cloud. This stage follows [8] but separates the latent (intended for reconstruction) and sparse priors (intended for storage) to relax the size constraints on the latents and reduce the redundancy of the latents. The second stage aims to get a comprehensive yet more compact sparse priors to latent denoising. Firstly, we sample sparse points and attached features to capture the structure surrounding each sparse latent point. To enable a larger receptive field and complement downsampling loss, we predict local distribution that describes the semantic context details, such as underlying surfaces, curvature, and point density. In this way, sparse priors are decoupled into intra-point and inter-point signals.

Sparse coding: Our DSP-DCM begins with a point encoder that maps the input point cloud to latent points X_L and features F_L . Despite the abstract transformation of large point clouds into latent space, the lack of distinction in the extracted latents leads to redundancy, resulting in unnecessary storage overhead. To address this problem, we aim to learn a more compact representation of the original point cloud. Rather than directly coding and storing the latents, we store a sparser representation that is obtained via a separate encoder Θ_S , which has a much higher down-sampling rate. The sparse representation captures the skeleton of the

3D shape, representing its global structure and local geometric details.

During decompression, we begin with a randomly initialized Gaussian noise and apply our PACD to reconstruct the latents, with the sparse representations serving as the conditions. The reconstructed latents are then fed into the decoder to generate high-fidelity point cloud. We adapt the auto-encoder architecture from D-PCC [8] for our application. Further details regarding model architecture are provided in the supplementary material.

Prior decoupling: Initially, the sparse representations are sampled as sparser point cloud $X_S = \{x_{S,i} \in \mathbb{R}^3 | 1 \leq i \leq N_S\}$ with associated features $F_S = \{f_{S,i} \in \mathbb{R}^3 | 1 \leq i \leq N_S\}$. The sparse points are then quantized and shifted to a non-negative point cloud $\hat{X}_S = \{\hat{x}_{S,i} \in \mathbb{N}^3 | 1 \leq i \leq N_S\}$, which is subsequently coded to bitstring and decoded back by an entropy model \mathcal{E} . The sparse points summarize the collapsed points surrounding them, which are discarded during downsampling. This encoding captures the relationships within the collapsed set around each sparse latent point, but neglects the spatial dependencies among the sparse latent points themselves, which may degrade reconstruction quality.

To get a more compact and comprehensive representation, we derive a local distribution feature explicitly,

$(\mu_S, \sigma_S) = \{(\mu_i, \sigma_i) | \mu_i \in \mathbb{R}, \sigma_i \in \mathbb{R}\}$ for sparse points. This is achieved by a lightweight distribution predictor \mathcal{P} , which consists of stacked convolutional layers (which we will explain later in Sec 4.3). These sparse points and their local distributions are summarized as **sparse priors**, which are then embedded as conditions of the PACD detailed in Sec 3.2. Finally, the point decoder Ω_L reconstructs the original point cloud from denoised latents $\tilde{\mathcal{X}}_L$.

3.2. Progressive Attention-based Conditional Denoiser

Given the inevitable information loss during downsampling, the mapping from sparse points to latent points becomes ill-posed and prone to clustering artifacts in the reconstructed point cloud. To address this, we leverage diffusion models, known for their robust generative capabilities, to encapsulate variability inherent in original point cloud X , thereby preserving essential details and mitigating inherent outliers through iterative denoising steps.

To maintain high fidelity of the latents, our DCM incorporates sparse priors into the PCAD at each encoding and decoding stage throughout the denoising process. The reverse process of diffusion is modeled as a Markov chain, given by:

$$p_\theta(\mathbf{X}_{L,0}, \dots, \mathbf{X}_{L,T-1} | \mathbf{X}_{L,T}) = \prod_{t=1}^T p_\theta(\mathbf{X}_{L,t-1} | \mathbf{X}_{L,t}, \mathbf{X}_S). \quad (1)$$

The stepwise denoising follows a Gaussian distribution:

$$p_\theta(\mathbf{X}_{L,t-1} | \mathbf{X}_{L,t}, \mathbf{X}_S) = \mathcal{N}(\mathbf{X}_{L,t-1}; \mu_\theta(\mathbf{X}_{L,t}, \mathbf{X}_S, t), \sigma_t^2 \mathcal{I}), \quad (2)$$

and the mean $\mu_\theta(\mathbf{X}_{L,t}, \mathbf{X}_S, t)$ is reparameterized as

$$\mu_\theta(\mathbf{X}_{L,t}, \mathbf{X}_S, t) = \frac{1}{\sqrt{\alpha_t}} (\mathbf{X}_{L,t} - \frac{\beta_t}{\sqrt{1 - \alpha_t}} \epsilon_\theta(\mathbf{X}_{L,t}, \mathbf{X}_S, t)). \quad (3)$$

The noise is encapsulated by the denoising network ϵ_θ , and α_t and β_t are predefined small positive constants with $\alpha_t = 1 - \beta_t$, and the cumulative product $\bar{\alpha}_t = \prod_{i=1}^t \alpha_i$.

Our PCAD employs a U-Net-like architecture, with N_L layers in both the encoder and decoder. At each layer, the sparse point cloud is delicately fused to offer guidance. Each denoising layer processes an input point cloud $\tilde{\mathbf{X}}_{L,t}^l$, which is intentionally noised based on a pre-scheduled timestep t , where $1 \leq l \leq N_L$. Given that sparse points \mathbf{X}_S^l and latents $\tilde{\mathbf{X}}_L^l$ are both proper subsets of the original point cloud and share homogeneous characteristics, we safely concatenate them along the point dimension. Note that \mathbf{X}_S^l is acquired by aligning the feature dimensions of \mathbf{X}_S by an MLP for each layer. After using an MLP layer to extract point-wise features from concatenated inputs $(\tilde{\mathbf{X}}_L^l, \mathbf{X}_S^l)$, we rely on an improved set abstraction layer [15] to filter out redundant geometric information while preserving essential

geometry and semantic candidates. This results in a coarse prediction $\tilde{\mathbf{F}}_L^{l-1}$ for $(l-1)_{th}$ layer.

We hypothesize that local distribution within the sparse point captures essential inter-point contextual information, which plays a pivotal role in enhancing the accuracy of our coarse predictions. We design a plug-in distribution predictor in the sparse encoder of DCM to predict the local distribution (μ_S, σ_S) and employ a cross-attention mechanism to integrate it with the coarse latent for scalability and explicitness. Using $\tilde{\mathbf{F}}_L^{l-1}$ as query, \mathbf{X}_S^{l-1} as key and $(\mu^{l-1}, \sigma^{l-1})$ as value, we are able to propagate the sparse distribution to latents, yielding a distribution-enhanced output $\tilde{\mathbf{F}}_L^{l-1}$.

Through iterative downsampling and fusion, we obtain refined features for the latents. The decoder part of the denoiser follows a similar scheme, with the set abstraction replaced by the feature mapper layer (detailed in supplementary material).

3.3. Context-aware Entropy Model

Recall that we derive the local distribution (μ_S, σ_S) upon the sparse points to provide extra guidance in the latent denoising process. We further utilize it to capture the coherent spatial dependencies within X_S during binarization by a naive bottleneck model \mathcal{P} .

Before \mathcal{P} , we first transform the sparse points X_S to enhance local features, which can be transformed back to point features using a synthesis transform during decompression. During compression, the X_S is transformed to Y_S in analyzed space:

$$\mathcal{G}_a : X_S \mapsto Y_S, \quad (4)$$

after being quantized and shifted to \hat{Y}_S , the non-negative \hat{Y}_S is coded to bitstring. During decompression, \hat{Y}_S is decoded back from bitstring, and \tilde{X}_S is obtained via symmetric synthesis transform to recover the sparse points:

$$\mathcal{G}_s : \hat{Y}_S \mapsto \tilde{X}_S. \quad (5)$$

Our distribution predictor \mathcal{P} consists of an analysis transform \mathcal{H}_a , a quantizer, and a synthesis transform \mathcal{H}_s . More expressively, the hyperparameter Z_S is obtained by an analysis transform:

$$\mathcal{H}_a : Y_S \mapsto Z_S. \quad (6)$$

After being quantized to \hat{Z}_S , the distribution parameters are obtained by a synthesis transform:

$$\mathcal{H}_s : \hat{Z}_S \mapsto (\mu_S, \sigma_S). \quad (7)$$

This is made differentiable by adding a uniform noise [1] during training. For simplicity, we will discard the lower-case s , which means sparse samples when discussing the distribution of \hat{Z}_S and \hat{Y}_S .

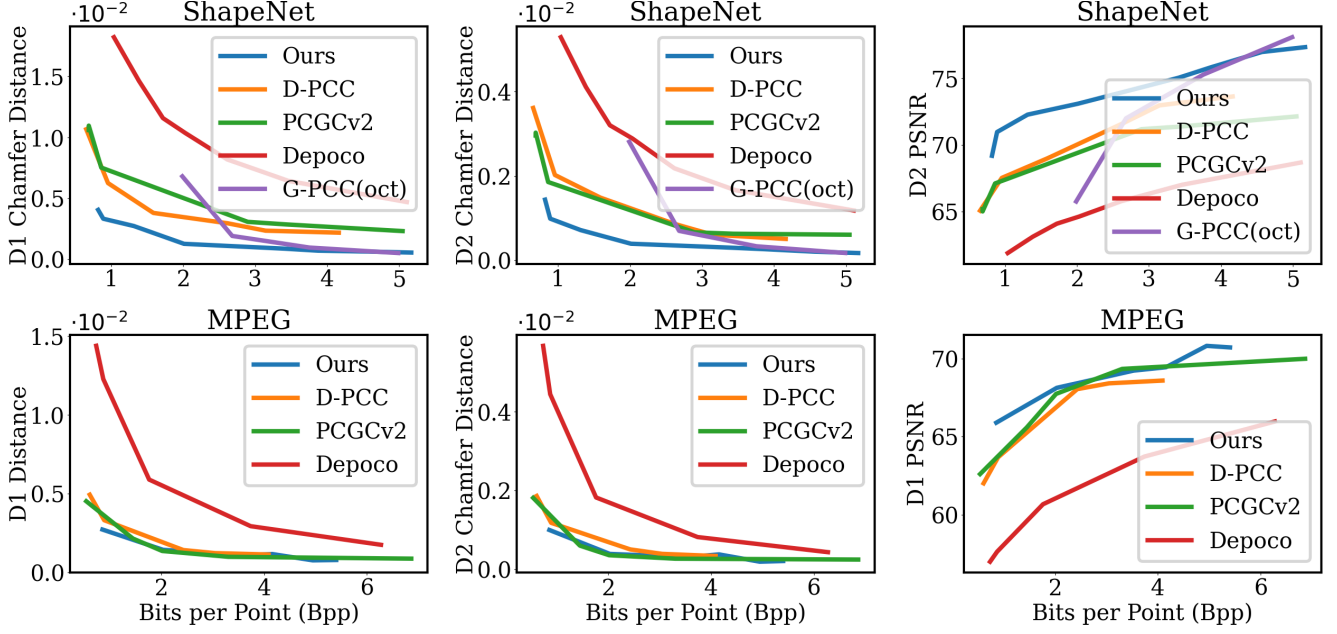


Figure 3. Quantitative result on ShapeNet and MPEG datasets.

Inspired by hyperprior-based context model in image compression [2, 17] and point cloud compression [29], we integrate \hat{Z}_S as priors into non-parametric, fully factorized density model

$$p_{\tilde{z}|\phi}(\tilde{z}|\Phi) = \prod_i (p_{\tilde{z}_i|\Phi^{(i)}}(\Phi^i) * \mathcal{U}(-\frac{1}{2}, \frac{1}{2}))(\tilde{z}_i). \quad (8)$$

So the distribution of each analyzed sparse point can be modelled as independently conditioned on the priors by convolving the *uniform* distribution introduced by quantization and *Laplace* distribution:

$$p_{\hat{y}_i|\hat{\mu}_i, \hat{\sigma}_i}(\hat{y}_i|\hat{\mu}_i, \hat{\sigma}_i) = \prod_i (\mathcal{L}(\hat{\mu}_i, \hat{\sigma}_i) * \mathcal{U}(-\frac{1}{2}, \frac{1}{2}))(\hat{y}_i). \quad (9)$$

After predicting the sparse points by saved \mathcal{P} , the arithmetic coder code \hat{Y}_S to bitstring and decode bitstring back to \hat{Y}_S according to local probability density function

$$p_{\hat{y}_i|\hat{\mu}_i, \hat{\sigma}_i}(\hat{y}_i|\hat{\mu}_i, \hat{\sigma}_i) = \int_{\hat{y}_i - \frac{1}{2}}^{\hat{y}_i + \frac{1}{2}} \mathcal{L}(y|\hat{\mu}_i, \hat{\sigma}_i) dy. \quad (10)$$

3.4. Loss Function

Firstly, we pre-train the encoder Θ_L and decoder Ω_L using the Chamfer Distance (CD) loss only.

$$CD(P, \hat{P}) = \frac{1}{|P|} \sum_i \min_j \|p_i - \hat{p}_j\|^2 \quad (11)$$

Then we train the diffusion model to learn the noise ϵ , the reconstruction loss is given by

$$\mathcal{L}_{recon} = \mathcal{E}_{(X_L, X_S) \sim P_{data}} \|\epsilon - \epsilon_{\theta}(\sqrt{\alpha_t}X_L + \sqrt{1 - \alpha_t}\epsilon, X_L, X_S)\|^2 \quad (12)$$

For compression loss L_{comp} , the bits per points (Bpp) is approximated by the likelihood of sparse points and distributions, namely $E_{\hat{Y}_S}[-\log_2(p_{\hat{Y}_S}(\hat{Y}_S))]$ and $E_{\hat{Z}_S}[-\log_2(p_{\hat{Z}_S}(\hat{Z}_S))]$.

The final loss of denoiser is a weighted sum of two losses.

$$\mathcal{L} = \mathcal{L}_{recon} + \lambda_{comp} \cdot L_{comp} \quad (13)$$

4. Experiments

4.1. Experimental Setup

Datasets. Shapenet dataset [4] contains diverse polygonal models gathered from online CAD model repositories. We adopt the version pre-processed by [21], which contains 30661 object-level point clouds from 13 categories, and we followed the official training/testing split. We also use six test samples recommended by MPEG Group [7]. Specifically, we select *longdress*, *redandblack*, *loot*, and *solider* from 8iVFB [13], which represent static scenes. Additionally, we include *basketball_player* and *dancer* from OwlII [36], which offer point clouds of dynamic scenes. We sample $N = 2048$ points for each point cloud as the original input.

4.1.1. Evaluation Metrics.

Following previous methods [8, 31], we use Chamfer Distance (CD), PSNR, and BD-Rate [3] to evaluate the geometry accuracy and bits per point (Bpp) to evaluate the compression ratio. For all of metrics, we report both point-to-point (D1) and point-to-plane (D2) measurements. A

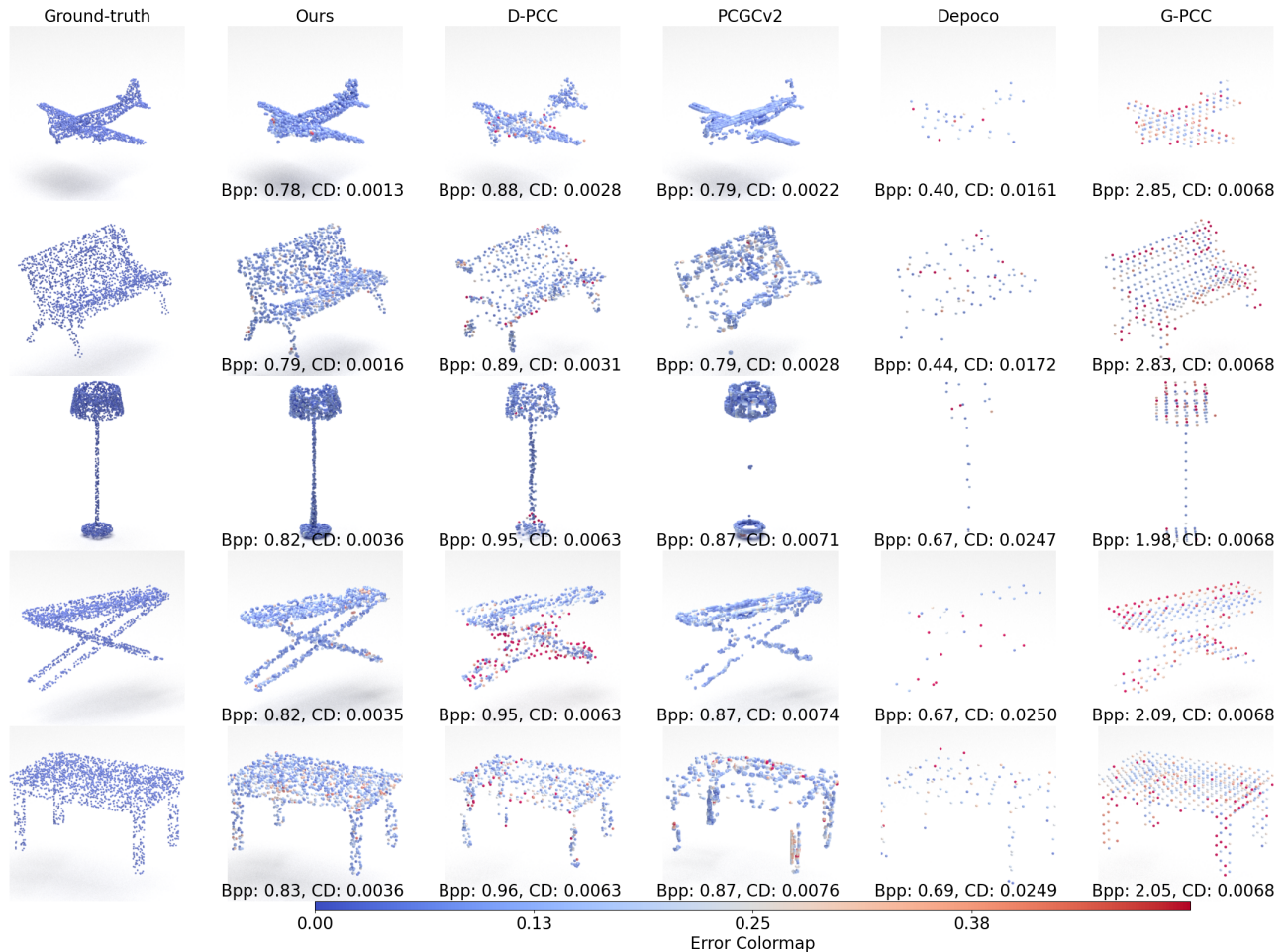


Figure 4. Qualitative comparison on the ShapeNet dataset, ensuring a consistent bits-per-point (bpp) across all methods.

lower bpp corresponds to a higher compression ratio, which means less space is needed for transmission and storage.

4.1.2. Baselines.

We choose three state-of-the-art deep-learning-based lossy point cloud compression methods: D-PCC [8], PCGCv2 [28], Depoco [32], and the common test condition TMC13-v25.0 of G-PCC [7] by MPEG PCC Group.

4.2. Experimental Results

Results for ShapeNet Compression. The rate-distortion curve is depicted on the left half of Fig. 3. For a fair comparison, all deep learning methods were trained on ShapeNet using only geometric coordinates. Our approach surpasses other baseline methods across all compression rates and exhibits significantly lower reconstruction errors at lower bitrates. This suggests that our decoupled data flow effectively preserves key geometric information while reducing storage requirements. Table 1 presents the BD-Rate improvements over the baseline G-PCC. On average, our proposed DSP-DCM demonstrates BD-Rate gains of 32.3%

and 37.6% relative to G-PCC for point-to-point and point-to-plane PSNR metrics, respectively. Note that the subpar performance of Depoco is mainly attributed to its lack of attribute information during training and inference.

Results for MPEG Compression. On the right half of Fig. 3, we provide the rate-distortion performance of learnable compression methods. G-PCC is excluded from this comparison due to its inability to handle sparse inputs effectively. Our method surpasses other baselines in PSNR and delivers competitive results regarding Chamfer Distance.

Methods	G-PCC	Depoco	PCGCv2	D-PCC	Ours
D1 (↓)	0%	137.88%	4.37%	-30.3%	-32.3%
D2 (↓)	0%	81.5%	-33.2%	-26.6%	-37.6%

Table 1. BD-Rate gains of against G-PCC on ShapeNet.

Qualitative evaluation. Fig. 4 presents the decompressed point cloud and corresponding compression ratio. Our approach reconstructs a significantly more complete point cloud while relying on limited information from the com-

pressed sparse priors.

4.3. Ablation Study

Condition Fusion Strategy. We conduct an ablation study to evaluate different fusion strategies and the effectiveness of cross attention fusion (abbreviated as 'attn.') on ShapeNet benchmark with a fixed $N_S = 76$. In Table 2, the first line shows the result of using denoiser network as generator that take the sparse priors as input and output latents. While the single-step generator achieves a modest improvement in Chamfer Distance (CD), it requires significantly more storage than diffusion models. Furthermore, our results highlight the advantages of the proposed fusion strategy compared to simply replacing the first N_S latent points with sparse points. By retaining all the noisy latents and then sampling from the combined set of latent and sparse points, the *concatenation and convolution* strategy achieves a more comprehensive understanding of the overall structure, thereby preserving a greater number of key-points. Additionally, the use of progressive cross-attention during both downsampling and upsampling stages enhances the identification of potential points within noisy latent representations at both intra-point and inter-point levels.

Fuse↓	attn. ↓	Fuse↑	attn. ↑	Bpp	CD (e-3)
generator				4.12	2.5
replace				1.20	3.6
cat&conv				1.10	3.3
cat&conv ✓				1.03	3.1
cat&conv ✓ cat&conv				0.99	3.0
cat&conv ✓ cat&conv ✓				0.98	2.8

Table 2. Performance of different fusion strategies and attention blocks. Both metrics benefit from lower values. Fuse and att. columns show condition fusion strategy and whether attention fusion is used. ↓ and ↑ means downsampling and upsampling stage. Replace means simply replacing the first N_S noisy latent points with sparse points in the fusion block, which cat&conv means concatenating the sparse points with latent points and convolution is followed.

Inter-point distribution in the binary coding and PCAD.

Table 3 illustrates the advantages of incorporating inter-point local distribution in the binary coding of sparse points and PCAD. In the first and third blocks of the table, compared to MLP, convolution achieves higher compression ratios and reconstruction quality. In the first and third block of the table, we show that compared to MLP, convolution gets higher compression ratio and reconstruction quality. This improvement is attributed to the larger receptive field of convolutional layers, which allow for more accurate prediction of the local distribution. Although point clouds are unordered, we hypothesize that point order influences the

contextual distribution in binary coding, as the coding process is performed sequentially, point by point. The second block highlights that integrating local distribution within the progressive attention-based fusion block enhances both metrics, as inter-point dependencies help to emphasize potential key points from higher levels. The second and third blocks illustrate the advantages of using a context-aware entropy model for feature coding over points coding. This can be explained by the fact that points are naturally sparse and can be coded with minimal bits, but preserving the distribution increases storage requirements. For feature coding, the bits reduction compensates for the additional cost of storing the distribution. The final block shows the efficiency of local distribution in binary coding and PCAD, along with the optimal settings. By maintaining a consistent distribution size with the sparse points, binary coding efficiency is enhanced, resulting in a lower bits-per-point metric.

Predictor Baseblock	Dist. Predicted	Preserved Size	attn.	Bpp	CD (e-3)
MLP	Feat	–	–	1.35	4.7
Conv	Feat	–	–	1.22	3.5
Conv	Pt	✓	–	1.18	3.4
Conv	Feat	✓	–	1.10	3.4
Conv	Pt	✓	✓	1.05	3.1
MLP	Feat	–	✓	1.15	3.5
Conv	Pt	–	✓	1.33	3.7
Conv	Feat	–	✓	1.12	3.2
Conv	Feat	✓	✓	1.03	3.1

Table 3. Performance of entropy coding strategies and attention mechanism. The first row reports results encoding via a context-free entropy model without predicting local distribution. **Dist. Predicted** specifies if a context-aware entropy model is applied to sparse points (Pt) or features (Feat). **Preserved Size** indicates size of local distribution is preserved in the distribution predictor’s bottleneck.

5. Conclusion

We introduced a decoupled sparse priors guided compression framework(DSP-DCM). It addresses the inherent redundancy in the latents by decoupling latent points, used for high-fidelity reconstruction, from sparse priors, used for efficient storage and transmission. By leveraging a progressive attention-based conditional denoiser (PACD), DSP-DCM enhances latent reconstruction with sparse priors. DSP-DCM also integrates a context-aware entropy model for optimal binary coding, which ensures minimal data loss and maintains high geometric and semantic integrity. Evaluations on the ShapeNet dataset and MPEG datasets confirm that DSP-DCM achieves state-of-the-art rate-distortion performance.

6. Acknowledgement

This research was supported by the Australian Research Council (ARC) under discovery grant project # 240101926. Professor Ajmal Mian is the recipient of an ARC Future Fellowship Award (project # FT210100268) funded by the Australian Government. This work is also partly supported by the National Natural Science Foundation of China under Grant 62373293.

References

- [1] Johannes Ballé, Valero Laparra, and Eero P Simoncelli. End-to-end optimized image compression. *arXiv preprint arXiv:1611.01704*, 2016. 5
- [2] Johannes Ballé, David Minnen, Saurabh Singh, Sung Jin Hwang, and Nick Johnston. Variational image compression with a scale hyperprior. *arXiv preprint arXiv:1802.01436*, 2018. 6
- [3] Gisle Bjontegaard. Calculation of average psnr differences between rd-curves. *ITU SG16 Doc. VCEG-M33*, 2001. 6
- [4] Angel X. Chang, Thomas Funkhouser, Leonidas Guibas, Pat Hanrahan, Qixing Huang, Zimo Li, Silvio Savarese, Manolis Savva, Shuran Song, Hao Su, Jianxiong Xiao, Li Yi, and Fisher Yu. ShapeNet: An Information-Rich 3D Model Repository, 2015. arXiv:1512.03012 [cs]. 6
- [5] Christopher Choy, JunYoung Gwak, and Silvio Savarese. 4d spatio-temporal convnets: Minkowski convolutional neural networks. In *Proceedings of the IEEE/CVF conference on computer vision and pattern recognition*, pages 3075–3084, 2019. 1
- [6] Chunyang Fu, Ge Li, Rui Song, Wei Gao, and Shan Liu. OctAttention: Octree-Based Large-Scale Contexts Model for Point Cloud Compression. *Proceedings of the AAAI Conference on Artificial Intelligence*, 36(1):625–633, 2022. Number: 1. 3
- [7] Danillo Graziosi, Ohji Nakagami, Satoru Kuma, Alexandre Zaghetto, Teruhiko Suzuki, and Ali Tabatabai. An overview of ongoing point cloud compression standardization activities: Video-based (v-pcc) and geometry-based (g-pcc). *AP-SIPA Transactions on Signal and Information Processing*, 9: e13, 2020. 6, 7
- [8] Yun He, Xinlin Ren, Danhang Tang, Yinda Zhang, Xi-angyang Xue, and Yanwei Fu. Density-preserving deep point cloud compression. In *Proceedings of the IEEE/CVF Conference on Computer Vision and Pattern Recognition*, pages 2333–2342, 2022. 2, 3, 4, 6, 7
- [9] Geoffrey E Hinton and Ruslan R Salakhutdinov. Reducing the dimensionality of data with neural networks. *science*, 313(5786):504–507, 2006. 3
- [10] Jonathan Ho, Ajay Jain, and Pieter Abbeel. Denoising diffusion probabilistic models. *Advances in neural information processing systems*, 33:6840–6851, 2020. 3
- [11] Lila Huang, Shenlong Wang, Kelvin Wong, Jerry Liu, and Raquel Urtasun. OctSqueeze: Octree-Structured Entropy Model for LiDAR Compression. In *2020 IEEE/CVF Conference on Computer Vision and Pattern Recognition (CVPR)*, pages 1310–1320, Seattle, WA, USA, 2020. IEEE. 3
- [12] Tianxin Huang and Yong Liu. 3d point cloud geometry compression on deep learning. In *Proceedings of the 27th ACM international conference on multimedia*, pages 890–898, 2019. 1
- [13] Maja Krivokuca, Philip A Chou, and Patrick Savill. 8i voxelized surface light field (8ivslf) dataset. *ISO/IEC JTC1/SC29/WG11 MPEG, input document m42914*, 2018. 6
- [14] Shitong Luo and Wei Hu. Diffusion probabilistic models for 3d point cloud generation. In *Proceedings of the IEEE/CVF*

- Conference on Computer Vision and Pattern Recognition*, pages 2837–2845, 2021. 3
- [15] Zhaoyang Lyu, Zhifeng Kong, Xudong Xu, Liang Pan, and Dahua Lin. A conditional point diffusion-refinement paradigm for 3d point cloud completion. *arXiv preprint arXiv:2112.03530*, 2021. 5
- [16] Zhaoyang Lyu, Jinyi Wang, Yuwei An, Ya Zhang, Dahua Lin, and Bo Dai. Controllable mesh generation through sparse latent point diffusion models. In *Proceedings of the IEEE/CVF conference on computer vision and pattern recognition*, pages 271–280, 2023. 3
- [17] David Minnen, Johannes Ballé, and George D Toderici. Joint autoregressive and hierarchical priors for learned image compression. *Advances in neural information processing systems*, 31, 2018. 6
- [18] Dat Thanh Nguyen, Maurice Quach, Giuseppe Valenzise, and Pierre Duhamel. Learning-Based Lossless Compression of 3D Point Cloud Geometry. In *ICASSP 2021 - 2021 IEEE International Conference on Acoustics, Speech and Signal Processing (ICASSP)*, pages 4220–4224, 2021. ISSN: 2379-190X. 1, 2
- [19] Dat Thanh Nguyen, Maurice Quach, Giuseppe Valenzise, and Pierre Duhamel. Multiscale deep context modeling for lossless point cloud geometry compression, 2021. arXiv:2104.09859 [cs, eess]. 2
- [20] Alex Nichol, Heewoo Jun, Prafulla Dhariwal, Pamela Mishkin, and Mark Chen. Point-e: A system for generating 3d point clouds from complex prompts. *arXiv preprint arXiv:2212.08751*, 2022. 3
- [21] Songyou Peng, Chiyu Jiang, Yiyi Liao, Michael Niemeyer, Marc Pollefeys, and Andreas Geiger. Shape as points: A differentiable poisson solver. *Advances in Neural Information Processing Systems*, 34:13032–13044, 2021. 6
- [22] Charles R. Qi, Hao Su, Kaichun Mo, and Leonidas J. Guibas. PointNet: Deep Learning on Point Sets for 3D Classification and Segmentation, 2017. arXiv:1612.00593 [cs] version: 2. 2
- [23] Charles R. Qi, Li Yi, Hao Su, and Leonidas J. Guibas. PointNet++: Deep Hierarchical Feature Learning on Point Sets in a Metric Space, 2017. arXiv:1706.02413 [cs]. 2
- [24] Maurice Quach, Giuseppe Valenzise, and Frederic Dufaux. Learning Convolutional Transforms for Lossy Point Cloud Geometry Compression. In *2019 IEEE International Conference on Image Processing (ICIP)*, pages 4320–4324, 2019. arXiv:1903.08548 [cs, eess, stat]. 2
- [25] Erik Sandström, Yue Li, Luc Van Gool, and Martin R Oswald. Point-slam: Dense neural point cloud-based slam. In *Proceedings of the IEEE/CVF International Conference on Computer Vision*, pages 18433–18444, 2023. 1
- [26] Jiaming Song, Chenlin Meng, and Stefano Ermon. Denoising diffusion implicit models. *arXiv preprint arXiv:2010.02502*, 2020. 3
- [27] Rui Song, Chunyang Fu, Shan Liu, and Ge Li. Efficient hierarchical entropy model for learned point cloud compression. In *Proceedings of the IEEE/CVF Conference on Computer Vision and Pattern Recognition*, pages 14368–14377, 2023. 3
- [28] Jianqiang Wang, Dandan Ding, Zhu Li, and Zhan Ma. Multi-scale point cloud geometry compression. In *2021 Data Compression Conference (DCC)*, pages 73–82. IEEE, 2021. 1, 7
- [29] Jianqiang Wang, Hao Zhu, Haojie Liu, and Zhan Ma. Lossy point cloud geometry compression via end-to-end learning. *IEEE Transactions on Circuits and Systems for Video Technology*, 31(12):4909–4923, 2021. 1, 2, 6
- [30] Jianqiang Wang, Hao Zhu, Zhan Ma, Tong Chen, Haojie Liu, and Qiu Shen. Learned Point Cloud Geometry Compression. *IEEE Transactions on Circuits and Systems for Video Technology*, 31(12):4909–4923, 2021. arXiv:1909.12037 [cs, eess]. 2
- [31] Jianqiang Wang, Dandan Ding, Zhu Li, Xiaoxing Feng, Chuntong Cao, and Zhan Ma. Sparse tensor-based multi-scale representation for point cloud geometry compression. *IEEE Transactions on Pattern Analysis and Machine Intelligence*, 45(7):9055–9071, 2022. 6
- [32] Louis Wiesmann, Andres Milioto, Xieyuanli Chen, Cyrill Stachniss, and Jens Behley. Deep compression for dense point cloud maps. *IEEE Robotics and Automation Letters*, 6(2):2060–2067, 2021. 7
- [33] Zijie Wu, Yaonan Wang, Mingtao Feng, He Xie, and Ajmal Mian. Sketch and text guided diffusion model for colored point cloud generation. In *Proceedings of the IEEE/CVF International Conference on Computer Vision*, pages 8929–8939, 2023. 1, 3
- [34] Wei Yan, Shan Liu, Thomas H Li, Zhu Li, Ge Li, et al. Deep autoencoder-based lossy geometry compression for point clouds. *arXiv preprint arXiv:1905.03691*, 2019. 1
- [35] Zetong Yang, Li Chen, Yanan Sun, and Hongyang Li. Visual point cloud forecasting enables scalable autonomous driving. In *Proceedings of the IEEE/CVF Conference on Computer Vision and Pattern Recognition*, pages 14673–14684, 2024. 1
- [36] Yao Lu Yi Xu and Ziyu Wen. *Owlii Dynamic human mesh sequence dataset*. ISO/IEC JTC1/SC29/WG11 m41658, 120th MPEG Meeting, Macau, 2017. 6
- [37] Linqi Zhou, Yilun Du, and Jiajun Wu. 3d shape generation and completion through point-voxel diffusion. In *Proceedings of the IEEE/CVF international conference on computer vision*, pages 5826–5835, 2021. 3